IEEE Access
Multidisciplinary | Rapid Review | Open Access Journal

IEEE POWER & ENERGY SOCIETY SECTION

Received November 21, 2020, accepted December 1, 2020, date of publication December 4, 2020,
date of current version December 17, 2020.

Digital Object Identifier 10.1109/ACCESS.2020.3042467

Loss Minimization of Electrified Railway Traction Systems Using SVC Based on Particle Swarm Optimization

GYU-SUB LEE[1], (Member, IEEE), PYEONG-IK HWANG[2], (Member, IEEE), BYEONG-GON LEE[3], (Member, IEEE), AND SEUNG-IL MOON[4], (Senior Member, IEEE)

[1]Seoul National University Electric Power Research Institute (SEPRI), Seoul 08826, South Korea
[2]Department of Electrical Engineering, Chosun University, Gwangju 61452, South Korea
[3]Korea Railroad Corporation (Korail), Daejeon 34618, South Korea
[4]Department of Electrical and Computer Engineering, Seoul National University, Seoul 08826, South Korea

Corresponding author: Pyeong-Ik Hwang (hpi@chosun.ac.kr)

This work was supported in part by the Korea Agency for Infrastructure Technology Advancement (KAIA) grant funded by Ministry of Land, Infrastructure and Transport (Grant 20RTRP-B146041-03). And in part by the National Research Foundation of Korea (NRF) grant funded by the Korea Government (MSIT; Ministry of Science and ICT) under Grant 2019R1G1A110010912.

ABSTRACT In this paper, we propose a method to minimize the system losses of electrified railway traction systems by utilizing static var compensators (SVCs). We suggest a power flow analysis model for a railway system considering two types of SVC connections: line-to-ground and line-to-line connections. Furthermore, an optimal operation whose objective is to minimize the system loss is presented based on particle swarm optimization by utilizing the power flow calculation method. The proposed power flow model and optimal operation are verified using MATLAB and PSCAD simulation programs. An electrified railway traction system can be operated economically by exploiting the proposed method.

INDEX TERMS Auto-transformer, railway traction system, static var compensator, power flow analysis, particle swarm optimization.

NOMENCLATURE

INDICES

k	Indices of auto-transformers (ATs)
n	Indices of trains
r, i	Indices of real and imaginary values
m	Indices of particls swarm optimization (PSO)

VARIABLES

V_{Ck}, I_{Ck}	Voltage and current of AT k at catenary
V_{Rk}, I_{Rk}	Voltage and current of AT k at rail
V_{Fk}, I_{Fk}	Voltage and current of AT k at feeder
V_{TCn}, I_{TCn}	Voltage and current of train n at catenary
V_{TRn}, I_{TRn}	Voltage and current of train n at rail
I_{Tn}	Current injected to train n
I_{GC}, I_{GF}	Current injected from the network
I_{SC}	Output current of SVC at catenary
I_{SF}	Output current of SVC at feeder
Q_{SC}	Reactive power of SVC at catenary
Q_{SF}	Reactive power of SVC at feeder

CONSTANTS

N_{AT}, N_T	Number of ATs and trains
N_{it}	Number of iteration for PSO
N_{PSO}	Number of position vectors for PSO
$R_C + jX_C$	Impedance of catenary
$R_R + jX_R$	Impedance of rail
$R_F + jX_F$	Impedance of feeder
$P_{Tn} + jQ_{Tn}$	Load of train n
t_n	Ratio of train n position
ρ_1, ρ_2, ρ_3	Random variables
ω_1, ω_2, ω_3	Weighting factors for PSO
η	Weighting factor for balancing
C_m	Variation coefficient for PSO

VECTORS

$\mathbf{U}_m$	Velocity vector at iteration m
$\mathbf{P}_m$	Position vector at iteration m
$\mathbf{P}_{Pb}$	Current best position vector
$\mathbf{P}_{Gb}$	Global best position vector

I. INTRODUCTION

An electric locomotive in a railway traction system is a great source of negative sequence current, harmonic currents, and

The associate editor coordinating the review of this manuscript and approving it for publication was Feng Wu.

voltage level reduction because it can be represented by a line-to-line load with an unbalanced characteristic [1]. Therefore, exploiting static var compensators (SVCs) has been considered a promising method to mitigate problems regarding power quality in railway traction systems [2]–[6]. In [2]–[3], a constant AC voltage control function was investigated for a railway traction system. In [4], the feasibility of an SVC was investigated at different positions. In addition, compensation methods for a negative sequence current in a three-phase system were developed in [5] and [6]. However, while SVC is being exploited for various purposes in the conventional power network (i.e., system loss minimization, profit maximization, and operating cost minimization), studies on the operation of SVCs in railway traction networks are scarce.

An efficient way to utilize an SVC in a power system is to determine the reactive power outputs based on the optimization problem [7]. Various studies to find the optimal operating points of an SVC for conventional transmission or distribution networks have been suggested [8]–[14]. For example, in [8] and [9], optimization problems to minimize the system losses and maximize the profit of network operators were proposed. However, to the best of our knowledge, such methods have rarely been investigated for electrified railway traction systems.

The load flow calculation method should be investigated to derive the optimal operating points of SVCs in railway traction systems because it is used as a constraint in optimization problems. Several studies have proposed load flow calculation methods for railway traction systems [15]–[17]. In [15], a load flow calculation method considering multiple trains was presented, and simulation studies considering various situations were provided. In [16], detailed characteristics of trains were considered in the power flow calculation, such as the variation in load consumption according to the velocity and the reactive power compensation function of locomotives. In [17], a power flow calculation method using an admittance matrix model of an auto-transformer (AT) and Scott transformer was presented. However, in [15]–[17], the operation of SVCs was not considered in the power flow calculation.

In [18], an optimal control method for SVCs in a railway traction system was proposed. The objective of the method in [18] is to minimize system losses, and the reactive power reference is determined based on linearized equations of the railway traction system. However, SVC is only considered a line-to-ground reactive power compensating device, and the power flow calculation method considering SVC was not presented in [18]. Thus, further studies on power flow calculation considering the practical connection of an SVC in a railway system are required.

Here, we propose an SVC operation method to minimize the power loss in an electrified railway traction system. First, a power flow calculation method considering SVCs in a railway traction system is proposed. Then, an optimization procedure based on particle swarm optimization (PSO) is proposed. Specifically, in this study, two implementation schemes of SVCs are considered: a single SVC connecting catenary to ground and two SVCs connecting catenary to rail and feeder to rail. The novelty and contributions of the study are summarized as follows:

- A power flow calculation method of an AT-fed railway traction system considering the operation of SVCs is proposed. Furthermore, the proposed method considers two SVC connection schemes.
- A loss minimization method using SVCs in a railway traction system is proposed. The proposed optimization method is based on PSO.
- It is verified via a comparison of the results of the electro-magnetic transient program PSCAD that the proposed power flow analysis method emulates practical AT-fed railway traction systems.
- It is observed by comparing the proposed method and existing SVC control schemes that the proposed operation scheme reduces system losses.

The remainder of this paper is organized as follows. Section II investigates the configuration of an AT-fed railway traction system and an SVC connection method. Section III presents the power flow calculation method of the railway system considering SVCs. Section IV provides an optimization procedure to minimize system losses. Section V verifies the proposed methods using two simulation programs: MATLAB and PSCAD. Finally, Section VI provides the conclusions of this paper.

II. SYSTEM CONFIGURATION

A. AT-FED RAILWAY TRACTION SYSTEM

Fig. 1 shows the configuration of an electrified railway traction system fed by 5 ATs. There are three phases: catenary, rail, and feeder. The currents are injected from the transmission network via the Scott transformer at the catenary and feeder sides. Trains are connected between the catenary and the rail, and their positions change with time. An SVC is connected at the 5-th AT (AT #5), and a configuration of the connection is described in Section II-B. Note that all the voltage and current parameters are in the form of complex numbers.

B. CONFIGURATION OF SVC CONNECTION

Fig. 2 shows the configurations for implementing an SVC in a railway traction system. Fig. 2(a) presents a single line-to-ground connection of the SVC. In this scheme, a single SVC is installed at the 5-th AT and the current (I_{SC}) is only provided via the catenary line. In Fig. 2(a), the SVC is grounded and not connected to the rail. Most previous studies considering SVCs in an AT-fed railway traction system assumed a line-to-ground connection [2]–[4], [18]. As reactive current flows like an unbalanced load in this scheme, there may be a voltage deviation in the rail phase (i.e., a voltage increase in V_{R5}).

On the other hand, the line-to-line connection scheme, which is depicted in Fig. 2(b), provides reactive power to both

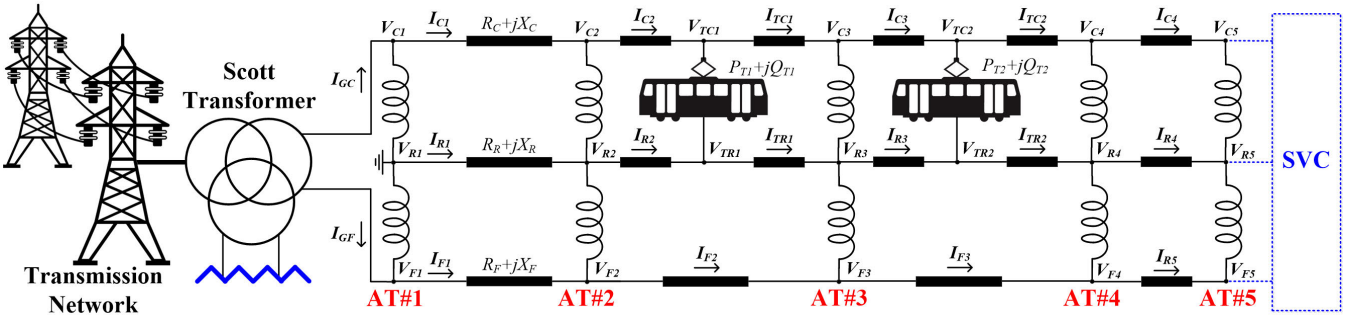

FIGURE 1. Configuration of a railway traction system fed by 5 ATs.

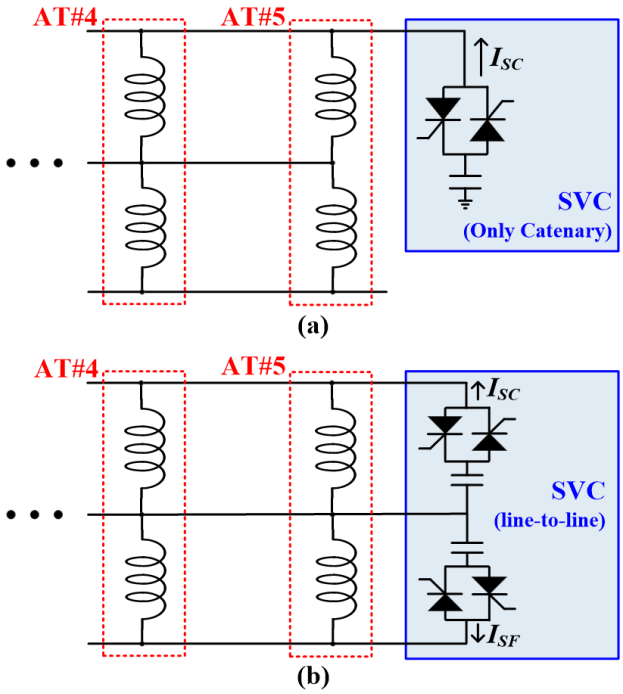

FIGURE 2. Configurations of SVC connections: (a) line-to-ground scheme and (b) line-to-line scheme.

the catenary and feeder. In addition, SVCs are not grounded and are connected to the rail phase. Therefore, in contrast to the line-to-ground scheme in Fig. 2(a), two SVCs are required to implement the system. In the line-to-line scheme, SVCs provide current to the catenary (I_{SC}) and feeder (I_{SF}), and the sum of the currents flows through the rail. As the current injected into the two sides can be regulated independently, this scheme is effective for load balancing (reducing negative current into the railway traction system) [19].

III. POWER FLOW CALCULATION MODEL

In this section, a power flow calculation model of an AT-fed railway traction system (described in Fig. 1) is presented, which is required for the optimal operation of SVCs. The two SVC connection methods described in Section II-B are considered in the model. To develop the calculation method, we first investigate simultaneous equations to represent the railway traction system and demonstrate that the proposed equations can be solved. Then, we propose a solution method.

A. EQUATIONS OF THE TRACTION SYSTEM

In Fig. 1, all the voltages and currents can be represented in the form of complex numbers. The real and imaginary parts of each variable are indicated by superscripts r and i, respectively (i.e., $I_{C1} = I^r_{C1} + jI^i_{C1}$). The railway traction system has two types of sections: sections with and without a train. Fig. 3(a) shows the configuration of the section without a locomotive between the catenary and the rail. In this case, the real and imaginary parts of the line current from the k-th AT to the $(k+1)$-th AT are defined, respectively, as

$$I^r_{xk} = \frac{R_x(V^r_{xk} - V^r_{x(k+1)}) + X_x(V^i_{xk} - V^i_{x(k+1)})}{R_x^2 + X_x^2}, \quad (1)$$

$$I^i_{xk} = \frac{R_x(V^i_{xk} - V^i_{x(k+1)}) - X_x(V^r_{xk} - V^r_{x(k+1)})}{R_x^2 + X_x^2}, \quad (2)$$

where $x \in \{C, R, F\}$. On the other hand, as shown in Fig. 3(b), the line currents of the catenary and rail sides flow from the k-th AT to the node connected to the train. Therefore, for the section including the train load, the real and imaginary parts of the line currents of the catenary and rail are, respectively, defined as

$$I^r_{yk} = \frac{R_y(V^r_{yk} - V^r_{Tyn}) + X_y(V^i_{yk} - V^i_{Tyn})}{t_n(R_y^2 + X_y^2)}, \quad (3)$$

$$I^i_{yk} = \frac{R_y(V^i_{yk} - V^i_{Tyn}) - X_y(V^r_{yk} - V^r_{Tyn})}{t_n(R_y^2 + X_y^2)}, \quad (4)$$

where $y \in \{C, R\}$. In addition, in this case, the real and imaginary parts of the line current flowing from the train side to the $(k+1)$-th AT can be defined, respectively, as

$$I^r_{Tyn} = \frac{R_y(V^r_{Tyn} - V^r_{y(k+1)}) + X_y(V^i_{Tyn} - V^i_{y(k+1)})}{(1-t_n)(R_y^2 + X_y^2)}, \quad (5)$$

$$I^i_{Tyn} = \frac{R_y(V^i_{Tyn} - V^i_{y(k+1)}) - X_y(V^r_{Tyn} - V^r_{y(k+1)})}{(1-t_n)(R_y^2 + X_y^2)}. \quad (6)$$

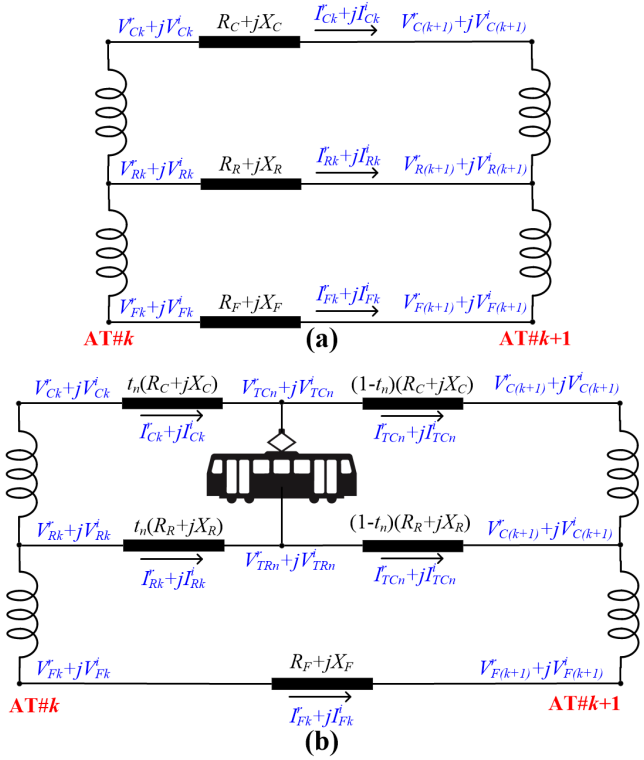

FIGURE 3. Configurations of the section between ATs (a) without a train and (b) with a train.

In addition, according to the characteristics of an AT, the currents from the rail to the catenary and feeder are identical. Therefore, the following equations can be defined at the catenary and feeder phases for the $k+1$-th AT in Fig. 3(a):

$$I^r_{Ck} + 0.5(I^r_{Rk} - I^r_{R(k+1)}) - I^r_{C(k+1)} = 0, \quad (7)$$
$$I^i_{Ck} + 0.5(I^i_{Rk} - I^i_{R(k+1)}) - I^i_{C(k+1)} = 0, \quad (8)$$
$$I^r_{Fk} + 0.5(I^r_{Rk} - I^r_{R(k+1)}) - I^r_{F(k+1)} = 0, \quad (9)$$
$$I^i_{Fk} + 0.5(I^i_{Rk} - I^i_{R(k+1)}) - I^i_{F(k+1)} = 0. \quad (10)$$

Note that (7)–(10) do not hold for AT #1 because the rail connected to the first AT is grounded (the injected current is not preserved). In the case of $k = 5$, the above equations change with the SVC connection method. Otherwise, the above equations can be described for the train in Fig. 3(b) as follows:

$$I^r_{TCn} + 0.5(I^r_{TRn} - I^r_{R(k+1)}) - I^r_{C(k+1)} = 0, \quad (11)$$
$$I^i_{TCn} + 0.5(I^i_{TRn} - I^i_{R(k+1)}) - I^i_{C(k+1)} = 0, \quad (12)$$
$$I^r_{Fk} + 0.5(I^r_{TRn} - I^r_{R(k+1)}) - I^r_{F(k+1)} = 0, \quad (13)$$
$$I^i_{Fk} + 0.5(I^i_{TRn} - I^i_{R(k+1)}) - I^i_{F(k+1)} = 0. \quad (14)$$

Then, as the voltages from the catenary to the rail and from the rail to the feeder are identical for an AT, the following equations are defined:

$$V^r_{Ck} + V^r_{Fk} - 2V^r_{Rk} = 0, \quad (15)$$
$$V^i_{Ck} + V^i_{Fk} - 2V^i_{Rk} = 0. \quad (16)$$

In Fig. 3(b), additional constraints can be defined by the characteristics of the train load. First, the power consumed by the n-th train satisfies the following equations:

$$P_{Tn} = (V^r_{TCn} - V^r_{TRn})I^r_{Tn} + (V^i_{TCn} - V^i_{TRn})I^i_{Tn}, \quad (17)$$
$$Q_{Tn} = (V^i_{TCn} - V^i_{TRn})I^r_{Tn} - (V^r_{TCn} - V^r_{TRn})I^i_{Tn}, \quad (18)$$

where

$$I^r_{Tn} + jI^i_{Tn} = (I^r_{Ck} + jI^i_{Ck}) - (I^r_{TCn} + jI^i_{TCn}), \quad (19)$$

In addition, the train current can be defined at the rail as:

$$I^r_{Tn} + jI^i_{Tn} = -(I^r_{Rk} + jI^i_{Rk}) + (I^r_{TRn} + jI^i_{TRn}). \quad (20)$$

Finally, for AT #1, the catenary and feeder are connected to the grid side and the rail is grounded, and the following equations are satisfied:

$$(V^r_{C1} + jV^i_{C1}) - (V^r_{F1} + jV^i_{F1}) = V_G, \quad (21)$$
$$V^r_{R1} + jV^i_{R1} = 0. \quad (22)$$

B. EQUATIONS OF SVC

As SVCs are implemented at AT #5, the current constraints regarding the 5-th AT change with the SVC connection scheme. For the single line-to-ground scheme depicted in Fig. 2(a), the currents at the catenary and feeder satisfy the following equations:

$$I^r_{C4} + 0.5I^r_{R4} + I^r_{SC} = 0, \quad (23)$$
$$I^i_{C4} + 0.5I^i_{R4} + I^i_{SC} = 0, \quad (24)$$
$$I^r_{F4} + 0.5I^r_{R4} = 0, \quad (25)$$
$$I^i_{F4} + 0.5I^i_{R4} = 0. \quad (26)$$

Furthermore, the output current should satisfy the following equations:

$$(V^r_{C5} + jV^i_{C5})(I^r_{SC} - jI^i_{SC}) = jQ_{SC}. \quad (27)$$

On the other hand, for the line-to-line connection mode depicted in Fig. 2(b), currents are injected into both the catenary and feeder. Furthermore, in contrast to the line-to-ground connection, the current flows from the rail phase. Therefore, (23)–(26) are modified as

$$I^r_{C4} + 0.5I^r_{R4} + 0.5I^r_{SC} = 0, \quad (28)$$
$$I^i_{C4} + 0.5I^i_{R4} + 0.5I^i_{SC} = 0, \quad (29)$$
$$I^r_{F4} + 0.5I^r_{R4} + 0.5I^r_{SF} = 0, \quad (30)$$
$$I^i_{F4} + 0.5I^i_{R4} + 0.5I^r_{SF} = 0. \quad (31)$$

Similar to the line-to-ground connection, the output currents (I^r_{SC}, I^i_{SC}, I^r_{SF}, and I^i_{SF}) satisfy the following conditions:

$$(V^r_{C5} - V^r_{R5})I^r_{SC} + (V^i_{C5} - V^i_{R5})I^i_{SC} = 0, \quad (32)$$
$$(V^i_{C5} - V^i_{R5})I^r_{SC} - (V^r_{C5} - V^r_{R5})I^i_{SC} = Q_{SC}, \quad (33)$$
$$(V^r_{F5} - V^r_{R5})I^r_{SF} + (V^i_{F5} - V^i_{R5})I^i_{SF} = 0, \quad (34)$$
$$(V^i_{C5} - V^i_{R5})I^r_{SF} - (V^r_{F5} - V^r_{R5})I^i_{SF} = Q_{SF}, \quad (35)$$

TABLE 1. Simultaneous equations.

Definition	Equations	Number
Common Equations		
Line current definition	(1)–(6)	$6N_{AT}+4N_T-6$
Current Constraints of AT	(7)–(14)	$4N_{AT}-8$
Voltage Constraints of AT	(15)–(16)	$2N_{AT}$
Train Power Constraints	(17)–(18)	$2N_T$
Train Current Constraints	(19)–(20)	$2N_T$
Grid Voltage Constraints	(21)–(22)	4
Total Number		$12N_{AT}+8N_T-10$
Single Line-to-ground System		
Current Constraints of AT #5	(23)–(26)	4
SVC Power Constraints	(27)	2
Total Number		6
Double Line-to-line System		
Current Constraints of AT #5	(28)–(31)	4
SVC Power Constraints	(32)–(35)	4
Total Number		8

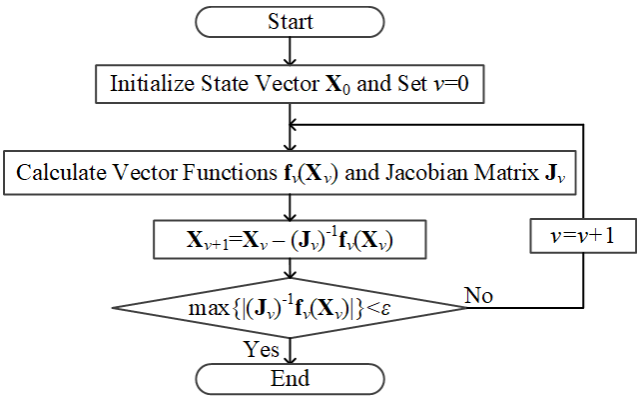

FIGURE 4. Flowchart of Newton–Raphson method.

C. SOLVING METHOD

As described in Sections III-A and III-B, (1)–(35) present the railway traction system with SVCs. There are $6N_{AT}+4N_T$ voltages and $6(N_{AT}-1)+4N_T$ line currents. In addition, two and four currents for SVCs are unknown for a single line-to-ground and line-to-line system, respectively. Note that the real and imaginary parts of the current and voltage are distinctive variables. Therefore, the total number of unknown variables is $12N_{AT}+8N_T-4$ for the line-to-ground scheme and $12N_{AT}+8N_T-2$ for the line-to-line scheme.

The equations defined by (1)–(35) are summarized in Table 1. As shown in Table 1, the numbers of unknown variables and simultaneous equations are identical for both cases. Thus, if the system is physically feasible, we can derive unique solutions. However, as (1)–(35) are non-linear equations, the Newton—Raphson method illustrated in Fig. 4 is utilized in this paper [20].

D. SCALABILITY OF THE PROPOSED METHOD

As the power flow calculation method was developed by generalized form, the calculation method can be adopted for not only the system described in Fig. 1 but also the railway traction system with the different number of ATs and trains. Furthermore, even if the method considered only one SVC at the last AT and two connection schemes, the power flow calculation with multiple SVCs or different connection method can be easily defined with small modification because a principle to make simultaneous equations is identical even for other topologies. Thus, it is suggested that the proposed method is scalable not only for the number of ATs and trains, but also for the number of SVCs and connection scheme.

IV. PROPOSED LOSS MINIMIZATION METHOD

A. PARTICLE SWARM OPTIMIZATION

PSO is an optimization method developed by Eberhart *et al.* [21]. It is a multi-agent search technique that has evolved from the emergent motion of a flock of birds searching for food. This technique has been widely used for optimization problems in power system applications [22]–[27]. For example, in [26], PSO was utilized to optimize combined heat and power system. Also, in [27], the algorithm was exploited to operate thyristor-controlled series capacitor (TCSC). In the implementation of the PSO algorithm, the position vector ($\mathbf{P}_m$) and velocity vector ($\mathbf{U}_m$) should be first defined at the current step (m). Then, the velocity and position at the next step can be calculated as follows:

$$\begin{aligned}\mathbf{U}_{m+1} &= \omega_1\mathbf{U}_m+\omega_2\rho_1\left(\mathbf{P}_{Pb}-\mathbf{P}_m\right)\\ &\quad+\omega_3\rho_2\left(\mathbf{P}_{Gb}-\mathbf{P}_m\right), \qquad (36)\\ \mathbf{P}_{m+1} &= \mathbf{P}_m+\mathbf{U}_{m+1}. \qquad (37)\end{aligned}$$

where ρ_1 and ρ_2 are random variables in the range [0,1].

To mitigate premature convergence of the proposed PSO algorithm. A mutation strategy described in [28] is utilized to maintain population diversity. Specifically, when premature convergence is detected during the iteration, the positions of particles are updated by adding random perturbations as:

$$\mathbf{P}_{m+1}=\mathbf{P}_m+C_m\rho_3(\max\left(\mathbf{P}_m\right)-\min\left(\mathbf{P}_m\right)), \qquad (38)$$

where, ρ_3 is random variable in the range [-0.5,0.5].

B. PROBLEM FORMULATION

The objective of the reactive power dispatch for SVCs is to minimize the active power loss in the railway traction system, which can be expressed as follows:

$$f_{obj}=V_{C1}^rI_{C1}^r+V_{F1}^rI_{F1}^r-\sum_{n=1}^{N_T}P_{Tn}. \qquad (39)$$

The two left-hand side terms in f_{obj} are the active powers injected from the grid side, and the third term is the total active power load. If the system is a line-to-line connection system, an additional term is added to the objective function

as follows:

$$f_{obj} = V_{C1}^r I_{C1}^r + V_{F1}^r I_{F1}^r - \sum_{n=1}^{N_T} P_{Tn} + \eta \, |Q_{SC} - Q_{SF}| \quad (40)$$

The last term in (40) is added to minimize the mismatch between the two reactive power outputs in the SVCs, which reduces the voltage imbalance in the railway traction system. The importance of reactive power output balancing is determined by the weighting factor, η.

A penalty function (f_p) is also added to the above objective functions to exclude the infeasible solution causing a voltage violation. The penalty function is defined in (41), as shown at the bottom of the page. In (41), M is a sufficiently large number, V_{ub} is the upper bound, and V_{lb} is the lower bound. If there is no violation in the voltages at the catenary and feeder, the value of f_p is zero; thus, the objective function can be minimized.

C. OVERALL PROCEDURE

Fig. 5 shows a flowchart of the overall procedure. First, N_{PSO} position vectors are generated randomly. Then, f_{obj} is calculated for each position vector and the best position is defined as $\mathbf{P}_{Pb}$ and $\mathbf{P}_{Gb}$. Furthermore, the value of the objective function for the best position is defined as f_{Pb} and f_{Gb}. When calculating f_{obj}, the power flow calculation method derived in Section III is exploited.

As shown in Fig. 5, the update of the position vectors is iterated N_{it} times. For each iteration number (m), f_{Pb} is derived. In addition, after calculating the best position and objective function value, velocity vectors are calculated and the next position vectors are derived using (36) and (37), respectively. Finally, if $m = N_{it}$, the iteration is completed and the optimal solution is derived. The detailed procedure for calculation and derivation is illustrated in Fig. 5.

Even the proposed optimization method is designed for one SVC at the last AT, the proposed method can be modified for the system including multiple SVCs with few efforts because increase in position vector size can be easily adopted for PSO, which is relative advantages of heuristic optimization method [25]. Thus, the proposed optimization method is also scalable for general railway traction system similar with the power flow calculation method.

V. SIMULATION RESULT

Two cases are investigated in this study for verification. The first case is investigated to verify the proposed power flow calculation method, which is described in Section V-A. In this case, the test system is identical to that in Fig. 1. Two trains are connected in the traction system; the first train is connected between ATs #2 and #3, and the second train is connected between ATs #3 and #4. The active and reactive power absorptions of the two trains are 8 MW and 2 MVAr, respectively. The two trains are located on the 3:4 section between the two ATs. The railway traction system is con-

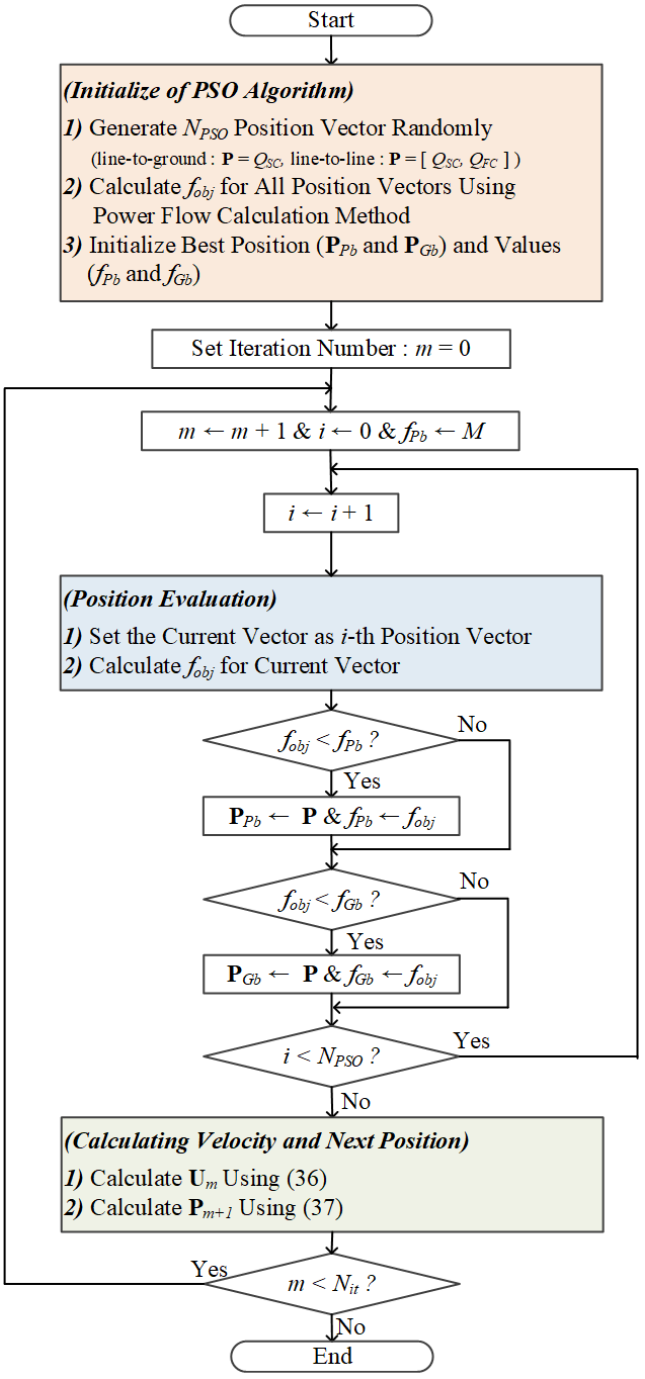

FIGURE 5. Overall procedure of the proposed method.

$$f_p = M\left[\sum_{k=1}^{N_{AT}} \max(V_{Ck} - V_{ub}, 0) + \sum_{k=1}^{N_{AT}} \max(V_{Fk} - V_{ub}, 0) + \sum_{k=1}^{N_{AT}} \max(V_{lb} - V_{Ck}, 0) + \sum_{k=1}^{N_{AT}} \max(V_{lb} - V_{Fk}, 0)\right]. \quad (41)$$

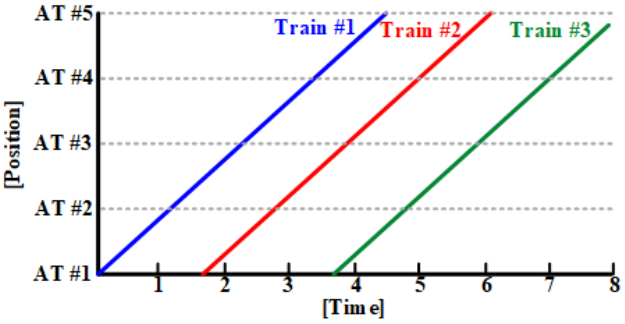

FIGURE 6. Positions of trains in Case 2.

nected to a 135 kV AC transmission network, and the turn ratio of the Scott transformer is 135:50 (i.e., $V_{C1} - V_{F1} = 50$ kV). The line impedances of the catenary, feeder, and rail between the ATs are $0.71 + j1.2241\ \Omega$, $0.71 + j1.2241\ \Omega$, and $2.4 + j3.5814\ \Omega$, respectively, which are derived from [29]. The simulation for the first case was performed using both PSCAD and MATLAB. In addition, both the SVC schemes in Fig. 2 are investigated.

In Section V-B, the second case is investigated to verify the proposed optimal operation method. All the parameters of the railway traction system are identical to those in the first case. The only difference is that three trains moving from AT #1 to AT #5 are considered, and their positions change according to time. Fig. 6 shows the positions of the trains according to the time period. In Section V-B, a MATLAB simulation is presented to compare the power losses between the railway traction systems with and without SVCs. Also, in Section V-C, to verify the proposed method for various conditions, 1,000 randomly generated cases are investigated using the conventional and the proposed method. The simulation was performed with following hardware specifications: Intel core i9-10900 @ 2.80 GHz, 64-bit, and 32 GB RAM.

A. VERIFICATION OF POWER FLOW ANALYSIS

Table 2 lists the results of the power flow calculation with a single line-to-ground connected SVC. In the case study, the output reactive power of the SVC (Q_{SC}) is 5 MVAr. As presented in Table 2, the voltage and current profiles for the results of PSCAD and MATLAB are almost identical. Specifically, the maximum errors for the voltage and current are 0.0023 kV and 0.0003 kA, respectively, which are only 0.0092 % and 0.075 % of the rated voltage and current levels, respectively. Therefore, for the railway traction system with a single line-to-ground connected SVC, it is suggested that the proposed power flow calculation method emulates the actual system well.

Table 3 lists the results of the power flow calculation with double line-to-line connected SVCs. In the case study, both outputs of SVCs at the catenary and feeder sides (Q_{SC} and Q_{SF}) are 3 MVAr. Similar to the result in the case of a single line-to-ground scheme, the voltage and current profiles for the two software programs are almost identical. The maximum errors for the voltage and current are 0.0004 kV and 0.0003 kA, respectively, which are 0.0016 % and 0.075 % of the rated voltage and current levels, respectively. The mismatch in the proposed method is smaller for the line-to-line scheme; however, the calculation is exact in both cases.

As shown in the power flow calculation result, the double line-to-line connection scheme is more effective for voltage balancing in the railway traction system; consequently, smaller negative currents are generated. On the other hand, the voltage of AT #5 in the catenary phase is 25.2317 kV for case 1 and 24.9252 kV for case 2. However, the reactive power supplied by the SVCs is 5 MVAr for case 1 and 6 MVAr (3 MVAr $\times 2$) for case 2. Thus, it was observed that the voltage supporting capability is higher for a single line-to-ground connected SVC scheme because the AC voltage increases more with less reactive power.

TABLE 2. Power flow calculation result with line-to-ground SVC.

Voltage of ATs						
AT#	$\lvert V_C\rvert$ [kV]		$\lvert V_R\rvert$ [kV]		$\lvert V_F\rvert$ [kV]	
	PSCAD	MATLAB	PSCAD	MATLAB	PSCAD	MATLAB
1	25.0000	25.0000	0.0000	0.0000	25.0000	25.0000
2	24.8756	24.8756	0.1210	0.1205	24.6712	24.6722
3	24.8553	24.8554	0.2414	0.2409	24.4433	24.4454
4	25.0070	25.0070	0.3623	0.3614	24.3876	24.3898
5	25.2317	25.2316	0.4829	0.4819	25.4050	24.4073
Current from ATs						
AT#	$\lvert I_C\rvert$ [kA]		$\lvert I_R\rvert$ [kA]		$\lvert I_F\rvert$ [kA]	
	PSCAD	MATLAB	PSCAD	MATLAB	PSCAD	MATLAB
1	0.3465	0.3462	0.0281	0.0279	0.3350	0.3349
2	0.4323	0.4320	0.2033	0.2031	0.2385	0.2383
3	0.2861	0.2860	0.2036	0.2037	0.0700	0.0698
4	0.1843	0.1842	0.0280	0.0279	0.0140	0.0140

TABLE 3. Power flow calculation result with line-to-ground SVC.

Voltage of ATs						
AT#	$\lvert V_C\rvert$ [kV]		$\lvert V_R\rvert$ [kV]		$\lvert V_F\rvert$ [kV]	
	PSCAD	MATLAB	PSCAD	MATLAB	PSCAD	MATLAB
1	25.0000	25.0000	0.0000	0.0000	25.0000	25.0000
2	24.8002	24.8005	0.0003	0.0001	24.8003	24.8005
3	24.7034	24.7037	0.0008	0.0006	24.7034	24.7037
4	24.7778	24.7781	0.0008	0.0004	24.7779	24.7781
5	24.9252	24.9253	0.0000	0.0000	24.9251	24.9253
Current from ATs						
AT#	$\lvert I_C\rvert$ [kA]		$\lvert I_R\rvert$ [kA]		$\lvert I_F\rvert$ [kA]	
	PSCAD	MATLAB	PSCAD	MATLAB	PSCAD	MATLAB
1	0.3304	0.3301	0.0002	0.0000	0.3301	0.3301
2	0.4222	0.4219	0.1933	0.1930	0.2420	0.2419
3	0.2631	0.2630	0.1931	0.1932	0.1243	0.1241
4	0.1204	0.1204	0.0001	0.0000	0.1205	0.1204

B. VERIFICATION OF LOSS MINIMIZATION

Three cases are compared to demonstrate that the proposed method successfully reduces active power loss in an AT-fed

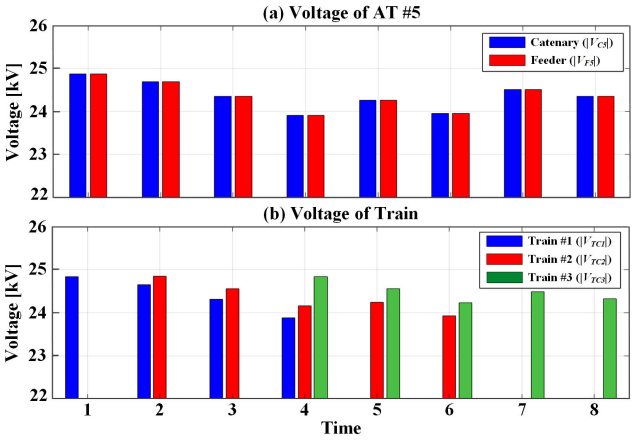

FIGURE 7. Simulation results without an SVC.

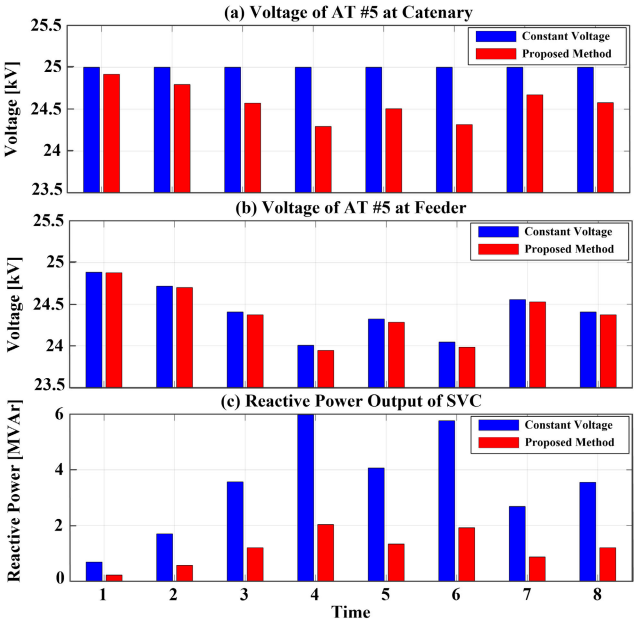

FIGURE 8. Simulation results with a single line-to-ground SVC.

railway traction system: a system without SVC, a single line-to-ground SVC, and line-to-line SVCs. For each case, 10 snapshots are investigated, as shown in Fig. 6. The time interval between two snapshots is 10 min. Fig. 7 shows the voltage profiles of the railway traction system without an SVC. As shown in Fig. 7(a), the voltages of the catenary and feeder were naturally maintained almost identical. The power loss without an SVC is 437.7 kWh during 80 min.

1) FOR THE SINGLE LINE-TO-GROUND SCHEME

Fig. 8 shows the simulation results for the same load profiles considering a single line-to-ground SVC. The results for the constant AC voltage control scheme and the proposed method are compared to demonstrate that the proposed method is more effective than the rule-based control scheme. As shown in Fig. 8(a), the AC voltage of AT #5 at the catenary was maintained at a nominal value (25 kV) regardless of the load profiles. On the other hand, for the proposed method, the magnitude of the AC voltage at the catenary changed according to time.

Fig. 8(b) shows the profile of the AC voltage at the feeder. As shown in Fig. 8(b), for the single line-to-ground SVC, the AC voltage magnitudes for the catenary and feeder were not balanced owing to the unbalanced reactive power provided by the SVC. From Figs. 8(a) and 8(b), it is observed that the voltage magnitudes were lower for the proposed method; thus, the reactive power provided by the SVC was also lower for the proposed method, as shown in Fig. 8(c). Therefore, it is suggested that the power loss is minimized and the capacity of the SVC is reduced by the proposed method for the railway traction system.

The active power losses for the voltage control and proposed methods were 465.50 kWh and 426.82 kWh, respectively. Although the AC voltage is maintained constant in the voltage control method, the power loss increases; consequently, the economic burden for the system operator may also increase. However, the active power loss is reduced by approximately 8.30 % by using the proposed method, and the voltage is maintained within the allowable range because the penalty factor is included in the objective function. The average elapsed time of the optimization is 4.92 sec for each time period, which is enough small to be implemented in practical application.

2) FOR THE DOUBLE LINE-TO-LINE SCHEME

Fig. 9 shows the simulation results for the double line-to-line SVCs. The scenario is identical to that of the single scheme. For the constant voltage control scheme in this case, the operation of the SVCs is decided by two rules: 1) maintaining the AC voltage at the catenary at the rated value and 2) maintaining the reactive power outputs for the two SVCs identical. As shown in Figs. 9(a) and 9(b), the voltage magnitudes are maintained at their nominal values for the constant voltage control scheme. In contrast to the single line-to-ground scheme, the AC voltages for the catenary and feeder are regulated simultaneously because the resources providing reactive power are located on both sides. In contrast, in the proposed method, the magnitude of the AC voltage changed according to the load profiles. Figs. 9(c) and 9(d) show the reactive power outputs for the two SVCs. Owing to the control objective of the voltage control mode, the reactive power outputs are the same for the two SVCs. However, the reactive power outputs for the proposed method are slightly different from each other because loss minimization is more important than power balancing.

The active power losses for the voltage control and proposed methods were 435.33 kWh and 417.21 kWh, respectively. The power loss of the constant voltage control scheme is higher than that of the single line-to-ground scheme. However, for the proposed method, the power loss is reduced

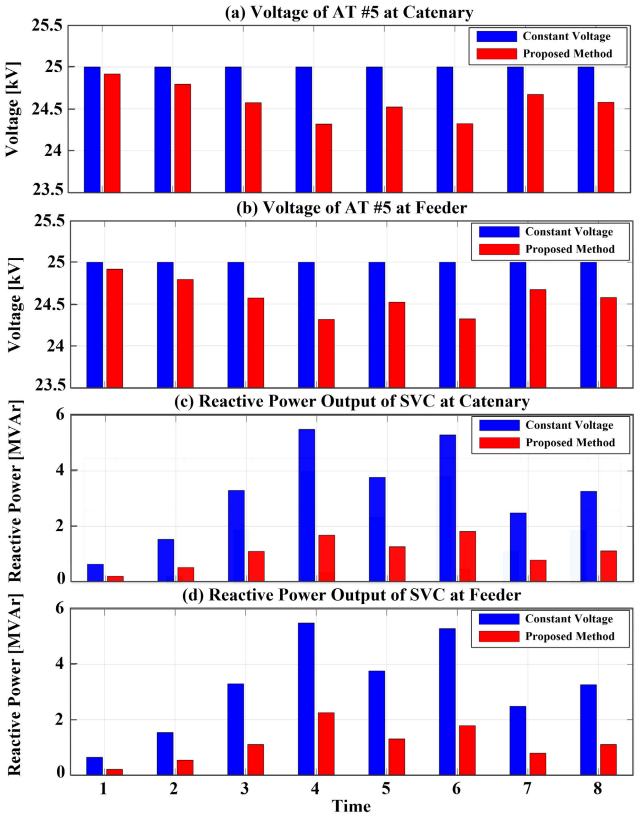

FIGURE 9. Simulation results with double line-to-line SVCs.

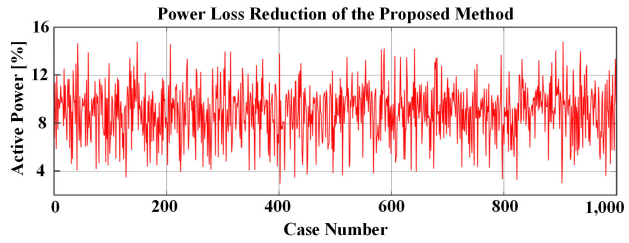

FIGURE 10. A statistical comparison for power losses between the constant voltage and the proposed method.

by 4.34 %, presumably due to the line-to-line connection scheme. The average elapsed time is 4.82 for double line-to-line scheme for each time period. Thus, the proposed method can be implemented in practical manner.

C. STATISTICAL ANALYSIS

To verify the proposed method for more generalized input data, statistical analysis for the power loss reduction is investigated. For the analysis, 1,000 randomly generated cases are utilized with variation in SVC connection scheme, train position, train number, and train load profile. Fig.10 shows the power loss reduction for the proposed method compared with the constant voltage control mode. As shown in Fig. 10, power losses of railway traction system are reduced for all cases. Maximum loss reduction in Fig. 10 is 14.77 % and minimum value is 2.99 %, thus, it is suggested that the performance of proposed method is statistically verified.

VI. CONCLUSION

In this paper, a PSO-based loss minimization method for an AT-fed railway traction system was presented. In addition, a new power flow calculation model considering an SVC was proposed. Two SVC connection schemes, single line-to-ground and double line-to-line, were considered in the power flow and optimization problem. The proposed method was verified using MATLAB and PSCAD simulations. Specifically, for power flow calculation model, the largest mismatch of voltage profile between MATLAB and PSCAD model is only 0.0092 %. Also, for the optimization method, power loss of railway traction system is reduced up to 14.77 %. Therefore, it is suggested that the proposed power flow model represent the railway traction system well and the proposed optimization method is effective for power loss reduction. In conclusion, SVCs can be exploited in a more efficient way for a railway traction system by using the proposed method.

REFERENCES

[1] L. Li, M. Wu, S. Wu, J. Li, and K. Song, "A three-phase to single-phase AC-DC-AC topology based on multi-converter in AC electric railway application," *IEEE Access*, vol. 7, pp. 111539–111558, Aug. 2019.

[2] G. C. Sekhar, V. S. Kale, and G. V. Krishna, "Application of SVC to improve voltage profile of indian railway traction system," in *Proc. IEEE Int. Conf. Power Electron., Drives Energy Syst. (PEDES)*, Dec. 2014, pp. 1–5.

[3] G. Celli, F. Pilo, and S. B. Tennakoon, "Voltage regulation on 25 kV AC railway systems by using thyristor switched capacitor," in *Proc. 9th Int. Conf. Harmon. Qual. Power.*, Oct. 2000, pp. 1–4.

[4] H. Wang, C. Zhang, K. Yan, Y. Fu, and Y. Liu, "Analysis of static VAr compensators installed in different positions in electric railways," *IET Electr. Syst. Transp.*, vol. 5, no. 3, pp. 129–134, Sep. 2015.

[5] Z. Guiping, C. Jianye, and L. Xiaoyu, "Compensation for the negative-sequence currents of electric railway based on SVC," in *Proc. 3rd IEEE Conf. Ind. Electron. Appl.*, Jun. 2008, pp. 1–6.

[6] J. Yuan, Y. Zhong, C. Zhang, W. Zeng, B. Chen, C. Tian, C. Deng, M. Zhou, K. Muramatsu, and J. Wang, "Optimal electromagnetic hybrid negative current compensation method for high-speed railway power supply system," *J. Modern Power Syst. Clean Energy*, vol. 4, no. 1, pp. 123–134, Jan. 2016.

[7] Y.-C. Chang, "Multi-objective optimal SVC installation for power system loading margin improvement," *IEEE Trans. Power Syst.*, vol. 27, no. 2, pp. 984–992, May 2012.

[8] J. Zhu, K. Cheung, D. Hwang, and A. Sadjadpour, "Operation strategy for improving voltage profile and reducing system loss," *IEEE Trans. Power Del.*, vol. 25, no. 1, pp. 390–397, Jan. 2010.

[9] B. Zhao, C. X. Guo, and Y. J. Cao, "A multiagent-based particle swarm optimization approach for optimal reactive power dispatch," *IEEE Trans. Power Syst.*, vol. 20, no. 2, pp. 1070–1078, May 2005.

[10] J. V. Milanovic and Y. Zhang, "Global minimization of financial losses due to voltage sags with FACTS based devices," *IEEE Trans. Power Del.*, vol. 25, no. 1, pp. 298–306, Jan. 2010.

[11] H. V. Padullaparti, Q. Nguyen, and S. Santoso, "Optimal placement and dispatch of LV-SVCs to improve distribution circuit performance," *IEEE Trans. Power Syst.*, vol. 34, no. 4, pp. 2892–2899, Jul. 2019.

[12] R. Minguez, F. Milano, R. Zarate-Minano, and A. J. Conejo, "Optimal network placement of SVC devices," *IEEE Trans. Power Syst.*, vol. 22, no. 4, pp. 1851–1860, Nov. 2007.

[13] R. Palma-Behnke, L. S. Vargas, J. R. Perez, J. Nunez, and R. A. Torres, "OPF with SVC and UPFC modeling for longitudinal systems," *IEEE Trans. Power Syst.*, vol. 19, no. 4, pp. 1742–1753, Nov. 2004.

[14] M. El-Azab, W. A. Omran, S. F. Mekhamer, and H. E. A. Talaat, "Allocation of FACTS devices using a probabilistic multi-objective approach incorporating various sources of uncertainty and dynamic line rating," *IEEE Access*, vol. 8, pp. 167647–167664, 2020.
[15] S. V. Raygani, A. Tahavorgar, S. S. Fazel, and B. Moaveni, "Load flow analysis and future development study for an AC electric railway," *IET Elect. Syst. Transp.*, vol. 2, no. 3, pp. 139–147, Sep. 2012.
[16] T. K. Ho, Y. L. Chi, J. Wang, K. K. Leung, L. K. Siu, and C. T. Tse, "Probabilistic load flow in AC electrified railways," *IEE Proc. Electr. Power. Appl.*, vol. 152, no. 4, pp. 1003–1013, Jul. 2005.
[17] H. Hu, Z. He, X. Li, K. Wang, and S. Gao, "Power-quality impact assessment for high-speed railway associated with high-speed trains using train timetable—Part I: Methodology and modeling," *IEEE Trans. Power Del.*, vol. 31, no. 2, pp. 693–703, Apr. 2016.
[18] T. Kulworawanichpong, "Optimising AC electric railway power flows with power electronic control," Ph.D. dissertation, Dept. Electron., Elect. Comput. Eng., Univ. Birmingham, Birmingham, U.K., 2003.
[19] *SVCs for Load Balancing and Trackside Voltage Control, ABB*. Accessed: Sep. 1, 2020. [Online]. Available: https://library.e.abb.com/public/c9f996d4f6c5c601c12570c9004b1754/A02-0196%20E%20LR.pdf
[20] A. R. Bergen and V. Vittal, *Power Systems Analysis*, 2nd ed. Upper Saddle River, NJ, USA: Prentice-Hall, 2000.
[21] Y. del Valle, G. K. Venayagamoorthy, S. Mohagheghi, J.-C. Hernandez, and R. G. Harley, "Particle swarm optimization: Basic concepts, variants and applications in power systems," *IEEE Trans. Evol. Comput.*, vol. 12, no. 2, pp. 171–195, Apr. 2008.
[22] M. Ramezani, M.-R. Haghifam, C. Singh, H. Seifi, and M. P. Moghaddam, "Determination of capacity benefit margin in multiarea power systems using particle swarm optimization," *IEEE Trans. Power Syst.*, vol. 24, no. 2, pp. 631–641, May 2009.
[23] J. Rodriguez-Garcia, D. Ribo-Perez, C. Alvarez-Bel, and E. Penalvo-Lopez, "Maximizing the profit for industrial customers of providing operation services in electric power systems via a parallel particle swarm optimization algorithm," *IEEE Access*, vol. 8, pp. 24721–24733, 2020.
[24] Z. Ren, H. Guo, P. Yang, G. Zuo, and Z. Zhao, "Bi-level optimization allocation of flexible resources for distribution network considering different energy storage operation strategies in electric market," *IEEE Access*, vol. 8, pp. 58498–58508, 2020.
[25] B. Yang, X. Cao, Z. Cai, T. Yang, D. Chen, X. Gao, and J. Zhang, "Unit commitment comprehensive optimal model considering the cost of wind power curtailment and deep peak regulation of thermal unit," *IEEE Access*, vol. 8, pp. 71318–71325, 2020.
[26] Y. Li, J. Wang, D. Zhao, G. Li, and C. Chen, "A two-stage approach for combined heat and power economic emission dispatch: Combining multi-objective optimization with integrated decision making," *Energy*, vol. 162, pp. 237–254, Nov. 2018.
[27] E. Naderi, M. Pourakbari-Kasmaei, and H. Abdi, "An efficient particle swarm optimization algorithm to solve optimal power flow problem integrated with FACTS devices," *Appl. Soft Comput.*, vol. 80, pp. 243–262, Jul. 2019.
[28] Y. Zhang, T. Li, G. Na, G. Li, and Y. Li, "Optimized extreme learning machine for power system transient stability prediction using synchrophasors," *Math. Problems Eng.*, vol. 2015, pp. 1–8, Sep. 2015.
[29] B. Mohamed, P. Arboleya, and M. Plakhova, "Current injection based power flow algorithm for bilevel 2 × 25kV railway systems," in *Proc. IEEE Power Energy Soc. Gen. Meeting (PESGM)*, Jul. 2016, pp. 1–5.

GYU-SUB LEE (Member, IEEE) received the B.S. and Ph.D. degrees in electrical engineering from Seoul National University, Seoul, South Korea, in 2013 and 2020, respectively. He is currently a Senior Researcher with the Seoul National University Electric Power Research Institute (SEPRI), Seoul. His research interests include control of HVDC systems and operation of railway traction systems.

PYEONG-IK HWANG (Member, IEEE) received the B.S. degree in science and the integrated M.S. and Ph.D. degree in electrical engineering from Seoul National University, Seoul, South Korea, in 2006 and 2014, respectively. From 2014 to 2015, he was a Research Professor with Korea University, Seoul. From 2015 to 2017, he was a Senior Researcher with the Korea Electric Power Research Institute, Daejeon, South Korea. He is currently an Associate Professor with Chosun University, Gwangju, South Korea. His research interests include distributed energy resources, distribution system operation, microgrids, smart grids, and railway traction systems.

BYEONG-GON LEE (Member, IEEE) is currently a Principal Researcher with the KORAIL Railroad Research Institute. His research interests include distributed energy resources, distribution system operation, microgrids, smart grids, and railway traction systems.

SEUNG-IL MOON (Senior Member, IEEE) received the B.S. degree in electrical engineering from Seoul National University, Seoul, South Korea, in 1985, and the M.S. and Ph.D. degrees in electrical engineering from Ohio State University, Columbus, OH, USA, in 1989 and 1993, respectively. He is currently a Professor with the School of Electrical and Computer Engineering, Seoul National University. His research interests include power system operation, power quality, HVDC systems, renewable energy, and distributed generation. He was a recipient of several awards and honors, including the Service Merit Medal (Korean Government), the Young-Moon Park Best Scholar Award, and the Outstanding Scholar Award (Korean Institute of Electrical Engineers).